Cement & Concrete Composites 45 (2014) 82–88

Contents lists available at ScienceDirect

Cement & Concrete Composites

journal homepage: www.elsevier.com/locate/cemconcomp

Reaction products and strength development of wastepaper sludge ash and the influence of alkalis

Gregor J.G. Gluth *, Christian Lehmann, Katrin Rübner, Hans-Carsten Kühne

BAM Federal Institute for Materials Research and Testing, Berlin, Germany

ARTICLE INFO

Article history:
Received 27 November 2012
Received in revised form 9 August 2013
Accepted 14 September 2013
Available online 21 September 2013

Keywords:
Wastepaper sludge ash
Reaction products
Monocarboaluminate
Strength
Alkali-activation

ABSTRACT

Wastepaper sludge ash (WSA) from a newsprint paper mill was investigated for its mineralogical composition and its reaction products and strength development after activation with water and sodium and potassium hydroxide solutions. The results showed the WSA to consist of calcite, free lime, gehlenite, tricalcium aluminate, belite, talc, quartz and probably a glassy phase. The principle reaction product was monocarboaluminate (CO_3–AFm) for the water- as well as for the alkali-activated WSA. Formation of monocarboaluminate and strength gain was more rapid for the alkali-activated WSA until 1 day of curing. However, afterwards reactions proceeded much slower when alkali solutions were used, leading to an about twice as high compressive strength for water-activated WSA mortars after 28 days of curing. The observed behavior is tentatively ascribed to a less uniform microstructure of the alkali-activated WSA. Significant differences between NaOH- and the KOH-activated WSA were not observed.

1. Introduction

In paper recycling, several types of waste sludge are produced; these sludges contain organics as well as inorganic fillers of the recycled paper (kaolin clay, calcium carbonate, talc, titanium dioxide). Part of them is reused in cement and ceramics industry, for soil improvement etc. [1]; a recent attempt is to produce metakaolin from the sludge by controlled calcination [2–4]. However, a large fraction of the sludge is still incinerated, which serves to recover energy and particularly to reduce the volume of waste material to be handled. The ashes generated in this process, often referred to as wastepaper sludge ash (WSA), differ widely in their chemical and mineralogical composition, depending on the composition of the feedstock, the production and waste treatment processes and the conditions of combustion [1,5]. Despite the volume reduction by incineration, the amount of waste, i.e. WSA, is still very large, which poses a significant problem to the paper industry, if no added-value application can be found for the WSA, i.e., if it has to be landfilled or otherwise handled entailing costs.

In this context, several studies investigated the use of WSA as cementitious material, either alone, in blends with Portland cement or mixed with other binder materials [6–13]. These studies confirmed that WSA generally possesses cementitious properties. Thus, in principle it may be used as binder or as supplementary cementitious material, which would not only reduce the amount of waste from paper industry to be landfilled, but would also contribute to lowered anthropogenic carbon dioxide emissions by partial replacement of Portland cement. However, only few studies [6,12,13] provided information about which compounds formed on hydration of WSA or blends containing WSA. Since the phase assemblage of the hardened pastes determines their mechanical properties and durability, it is essential to provide more data on the evolution of the reaction products, including the influence of specific compounds, which may be introduced intentionally or contained in the cementitious materials, used for mixing with the WSA. The present work aims to contribute to these issues by analyzing a WSA for strength development and reaction products after addition of water as well as after alkali-activation with sodium hydroxide and potassium hydroxide solutions.

2. Materials and methods

2.1. Starting materials

The wastepaper sludge ash (WSA) used as starting material in the present study was collected from a paper mill that produces newsprint, using exclusively recovered paper as raw material. It is a mixture of bottom ash and fly ash generated in co-combustion of sludge and smaller amounts of rejects from the recycling process and wood biomass in the fluidized bed of an on-site co-generation power station. Its main oxide composition and loss on ignition (LOI) are shown in Table 1. The fractions of CO_2 and free lime

* Corresponding author. Address: BAM Federal Institute for Materials Research and Testing, Unter den Eichen 87, 12205 Berlin, Germany. Tel.: +49 30 8104 3300; fax: +49 30 8104 1717.
E-mail address: gregor.gluth@bam.de (G.J.G. Gluth).

0958-9465/$ - see front matter © 2013 Elsevier Ltd. All rights reserved.
http://dx.doi.org/10.1016/j.cemconcomp.2013.09.009

Table 1
Chemical composition of the WSA.

Oxide	Amount in %
SiO_2	22.33
Al_2O_3	11.97
Fe_2O_3	0.59
TiO_2	0.36
CaO	44.18
MgO	2.42
Na_2O	0.24
K_2O	0.40
SO_3	3.64
Cl^-	0.45
LOI	13.34

(CaO_{free}) in the WSA were determined to be 11.7% and 10.3%, respectively. The mineralogical composition of the WSA is discussed in Section 3.1.

The WSA is generated and collected as powder, containing agglomerates of considerable size. It was ground shortly (6 s) in a vibratory disc mill to break up larger agglomerates. After this treatment, the particle size distribution of the WSA was: 100% < 351.5 μm, 90% < 125.8 μm, 50% < 16.6 μm, 10% < 1.8 μm (determined by laser granulometry, dispersion in propan-2-ol). The density of the WSA was determined to be 2.66 g cm^{-3}.

NaOH and KOH solutions of molar concentration 2 M were prepared from NaOH and KOH pellets (purissimum grade), respectively, and deionized water.

2.2. Paste samples

Pastes were prepared by addition of either deionized water (referred to as water-activated WSA), 2 M NaOH solution, or 2 M KOH solution (jointly referred to as alkali-activated WSA) to the WSA at a volume of liquid/mass of solid ratio of 1.00 cm^3 g^{-1} (equivalent to a water/solid ratio by mass of 1.00 for the water-activated paste). For the alkali-activated pastes this means that the amounts of Na_2O and K_2O in the samples were 6.2% and 9.4% by WSA weight, respectively. At volume of liquid/mass of solid ratios significantly lower than 1.00 cm^3 g^{-1} the pastes were not flowable enough to be mixed and cast without excessive air voids inside.

Mixing of the pastes was done manually. They were cast into cubes of edge length of 20 mm and cured in the moulds (not capped), stored in a closed box over an open water surface at 23 °C. After the desired curing time of 1, 3 or 7 days (and 28 days for the water-activated WSA) the hardened pastes were demoulded and dried by vacuum at a pressure <0.04 Pa and a temperature of 40 °C for 6–9 days (usually 7 days) and then stored in a desiccator over silica gel until required for testing. The mass loss after vacuum drying ranged from 55.0% to 68.6%, depending on activator and sample age.

2.3. Strength testing (paste samples)

For compressive strength determination the paste samples were tested using a 10 kN-testing machine at a loading rate of 240 N s^{-1}. Each strength value reported is the average of the results of five specimens.

2.4. X-ray diffraction analyses

For X-ray diffraction (XRD) analysis, the paste samples were ground in a vibratory disc mill. Powder diffraction patterns were recorded in $\theta/2\theta$ geometry in the range 3–63° 2θ at 1° min^{-1} (0.02° steps) [paste samples] or 4° min^{-1} (0.02° steps) [unhydrated WSA], using CuKα radiation. The X-ray tube operated at 40 kV and 40 mA. The specimen holder was rotated at 30 rpm during measurements to improve particle orientation statistics.

2.5. Thermogravimetric analyses

Thermogravimetric analyses were conducted on WSA and powdered paste samples of approximately 0.30 g at a constant heating rate of 5 K min^{-1} in flowing nitrogen. Recorded results are expressed as thermogravimetric (TG) and differential thermogravimetric (DTG) curves.

2.6. Mortar samples

For auxiliary strength tests, mortar samples were prepared from another batch of WSA from the same paper mill, with chemical composition (including CO_2 and CaO_{free}) very similar to that of the WSA, used for the tests described above. The WSA was not ground, since it was presumed that mixing together with aggregates would lead at least to a partial destruction of agglomerates.

For each kind of activator and curing time, a set of three prismatic test specimens 40 mm × 40 mm × 160 mm in size were prepared from 1350 g of CEN-standard sand (0–2 mm), 450 g of WSA and 405 cm^3 of activator (deionized water, 2 M NaOH or 2 M KOH solution). The presence of aggregates allowed the volume of liquid/mass of WSA ratio to be 0.90 cm^3 g^{-1}, i.e. lower than for the paste samples, at an acceptable workability. Mixing of the mortars was done in a mixer according to EN 196-1. The mortars were cast in two layers into steel moulds, vibrating the mould after casting each layer for 45 s. The moulds were covered with a plate of glass and stored in a closed box over an open water surface at 23 °C. After 24 h the specimens were demoulded and either immediately used for 1 day strength tests or put back into the closed box until the desired total curing time of 3, 7 or 28 days. The latter samples were subjected to strength testing directly after removal from the box, i.e. without drying, too. Flexural and compressive strength testing was conducted according to EN 196-1.

3. Results

3.1. Mineralogical composition of the WSA

From XRD analysis calcite ($CaCO_3$), lime (CaO), portlandite ($Ca(OH)_2$), talc ($Mg_3Si_4O_{10}(OH)_2$), gehlenite ($Ca_2Al(AlSi)O_7$) and quartz (SiO_2) are readily identified as crystalline compounds in the WSA (Fig. 1). In addition, the hump in the diffractogram at about 25–35° 2θ suggests the presence of an amorphous phase.

The reflection at glancing angle 33.3° 2θ is attributed to tricalcium aluminate ($Ca_3Al_2O_6$). This assignment is supported by the fact that the peak disappeared already after one day of hydration

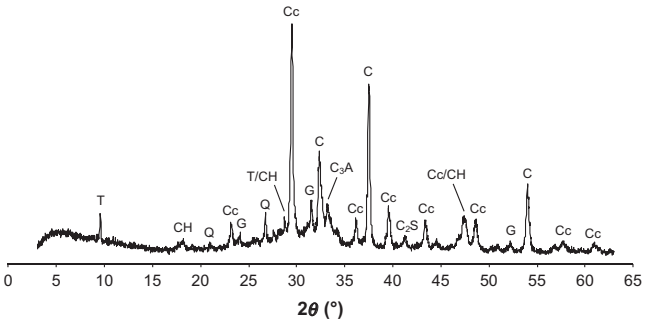

Fig. 1. Powder X-ray diffractogram (CuKα radiation) of the unhydrated WSA. Main peaks are labeled T: talc, CH: portlandite, Q: quartz, Cc: calcite, G: gehlenite, C: lime, C_3A: tricalcium aluminate, C_2S: belite.

(see Sections 3.2. and 3.3.), consistent with the high reactivity of tricalcium aluminate. A smaller peak at 41.2° 2θ indicates the presence of belite (β-Ca_2SiO_4). Other main peaks of this compound at about 32.2, 32.7, 36.8 and 37.5° 2θ appear to be superimposed by lime in the unhydrated WSA and partly by monocarboaluminate in the hydrated pastes (see Sections 3.2. and 3.3).

The thermogravimetric analysis of the WSA (Fig. 2) confirmed the presence of calcium carbonate (DTG peak at ~800 °C) and small amounts of portlandite (~410 °C). The portlandite in the WSA very likely originates from hydration of small quantities of free lime during transport and storage. The TG/DTG curves further indicate that virtually the complete amount of CO_2 in the WSA (11.7% according to wet chemical analysis) is bound as calcium carbonate. Based on this, the fraction of the latter in the WSA can be calculated to be about 27%.

3.2. Water-activated WSA

Fig. 3 shows the diffractograms of the WSA hydrated with water after different curing times up to 28 days. Peaks of calcite, portlandite, monocarboaluminate ($Ca_4Al_2(OH)_{12}CO_3{\cdot}5H_2O$, "$CO_3$–AFm") [14,15], quartz, gehlenite, belite and talc can be distinguished starting from the first day of hydration. The peaks of portlandite decreased with curing time and have disappeared after 28 days. Also, the reflection from belite at 41.2° 2θ becomes less pronounced with curing time and can no longer be distinguished after day 7. The peaks of lime and that related to tricalcium aluminate, both present for the unhydrated WSA, were absent for the hydrated pastes already after 1 day of hydration. The relative height of the monocarboaluminate main peak at 11.7° 2θ gradually increased with curing time, indicating its continuous formation.

The DTG curves of the hydrated pastes (Fig. 4) confirm the XRD results and give some information about the evolution of the phase assemblage. The peaks at about 460 °C and 775–800 °C are related to the thermal decomposition of portlandite and calcite, respectively. Portlandite is formed by reaction of the water with free lime at the beginning of the hydration. In the further course of the hydration, portlandite and calcite dissolved, shown by the diminishing of the respective peak heights. (The change in the amount of calcite is not apparent in the XRD results, Fig. 3. However, despite care in preparation and homogenization of the samples, it is most likely that this is caused by sampling effects.) At 28 days, virtually all portlandite was consumed. The peaks at 180–200 °C and about 250 °C as well as the shoulder at about 700–740 °C can be attributed to monocarboaluminate [2,16], formed by reaction of the dissolved calcium and carbonate with alumina from either tricalcium aluminate or the glassy phase of the WSA. These peaks are present already after one day and increased in course of the reaction, in particular from day 1 to day 3 of curing. From day 7 to day 28 a significantly slower formation of monocarboaluminate can be noted. The shoulder in the DTG curves around 100–120 °C can be assigned to either ettringite ($Ca_6Al_2(OH)_{12}(SO_4)_3{\cdot}nH_2O$) or C–S–H. Since no indications of ettringite were found from the XRD analyses, it is likely that the latter shoulder is related to C–S–H.

Strength results for the water-activated pastes are included in Fig. 5 and for the water-activated mortars in Fig. 6. Consistent with the development of the amount of monocarboaluminate until the seventh day of curing, the strengths of the paste and the mortar continuously increased until this curing time and afterwards rose more slowly. (For the water-activated paste, the compressive strength after 28 days of curing, not shown in Fig. 5, was 11.1 MPa).

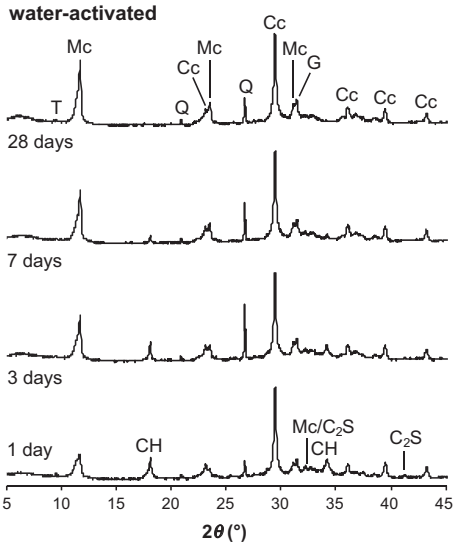

Fig. 3. Powder X-ray diffractograms (CuKα radiation) of the water-activated WSA after 1, 3, 7 and 28 days of curing. Main peaks are labeled T: talc, Mc: monocarboaluminate, CH: portlandite, Q: quartz, Cc: calcite, G: gehlenite, C_2S: belite.

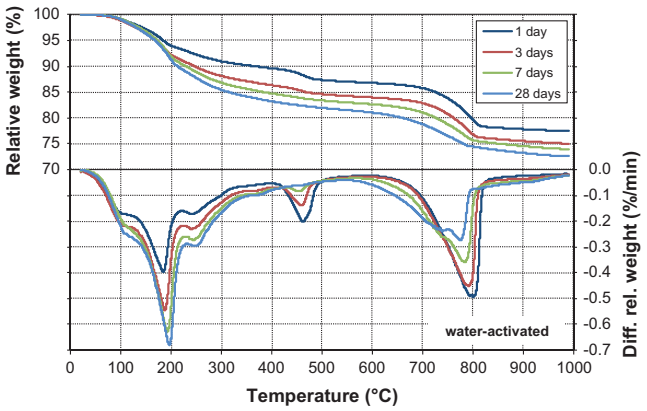

Fig. 4. TG/DTG curves of the water-activated WSA after 1, 3, 7 and 28 days of curing.

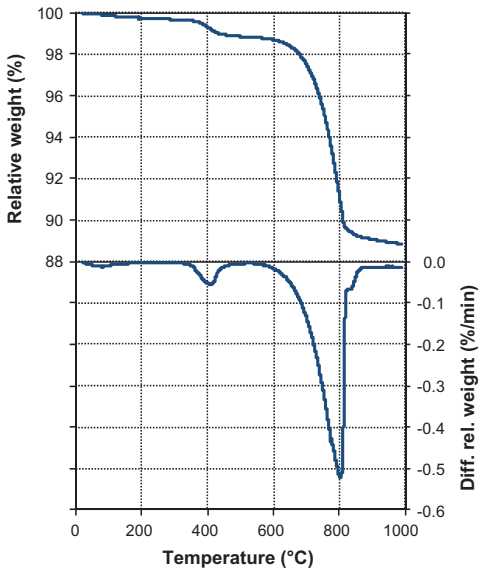

Fig. 2. TG/DTG curves of the unhydrated WSA.

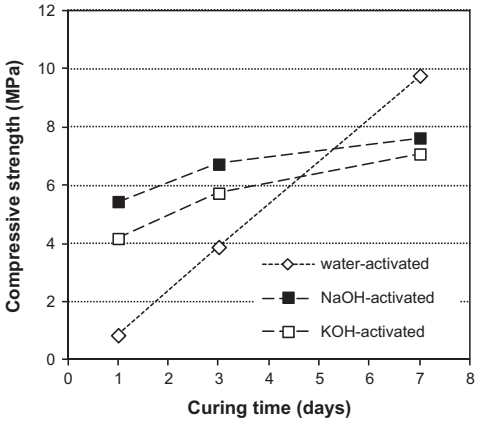

Fig. 5. Compressive strength of the WSA pastes. The compressive strength of the water-activated paste after a curing time of 28 days was 11.1 MPa (not shown).

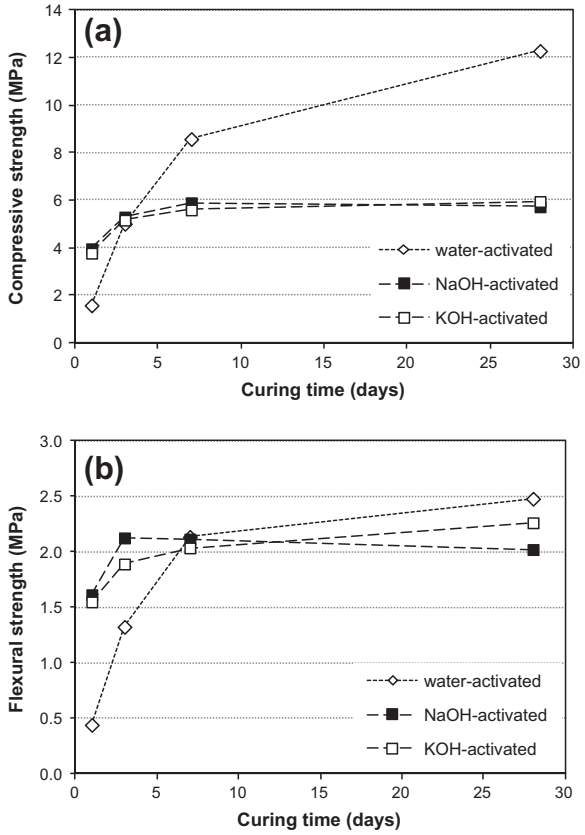

Fig. 6. Strengths of the WSA mortars: (a) compressive strength, (b) flexural strength.

3.3. Alkali-activated WSA

As shown in Figs. 7 and 8, the principle phases detected by XRD in the NaOH-activated and the KOH-activated pastes were the same as for the water-activated paste, viz. calcite, portlandite, monocarboaluminate, quartz, gehlenite, belite and talc were found. However, only small variations of the relative peak heights of monocarbonate as well as of calcite occurred, indicating only small changes in their amount from 1 to 7 days of curing. Since the carbonate ions in the monocarboaluminate, formed after 1 day, must come from the calcite of the WSA (Section 3.1), its formation proves that partial dissolution of calcite nevertheless took place during the first day of hydration. As with the water-activated

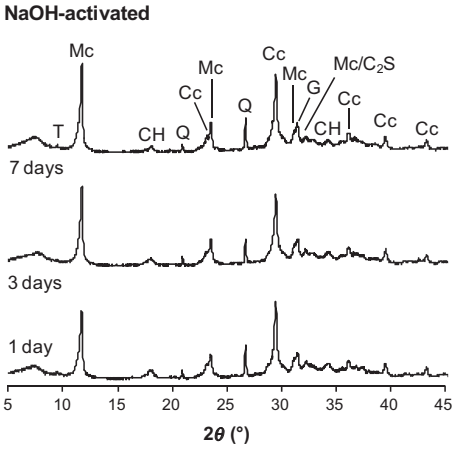

Fig. 7. Powder X-ray diffractograms (CuKα radiation) of the NaOH-activated WSA after 1, 3 and 7 days of curing. Main peaks are labeled T: talc, Mc: monocarboaluminate, CH: portlandite, Q: quartz, Cc: calcite, G: gehlenite, C_2S: belite.

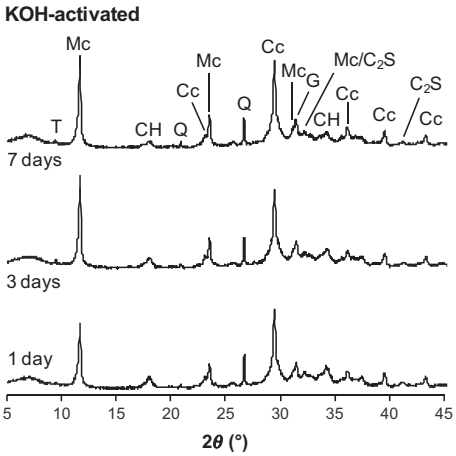

Fig. 8. Powder X-ray diffractograms (CuKα radiation) of the KOH-activated WSA after 1, 3 and 7 days of curing. Main peaks are labeled T: talc, Mc: monocarboaluminate, CH: portlandite, Q: quartz, Cc: calcite, G: gehlenite, C_2S: belite.

paste, peaks of lime and tricalcium aluminate were absent already after 1 day of curing.

Comparison of the step heights of the TG curves of the alkali-activated pastes (Figs. 9 and 10; assignment of DTG peaks/TG steps as for the water-activated paste, see Section 3.2.) with those of the

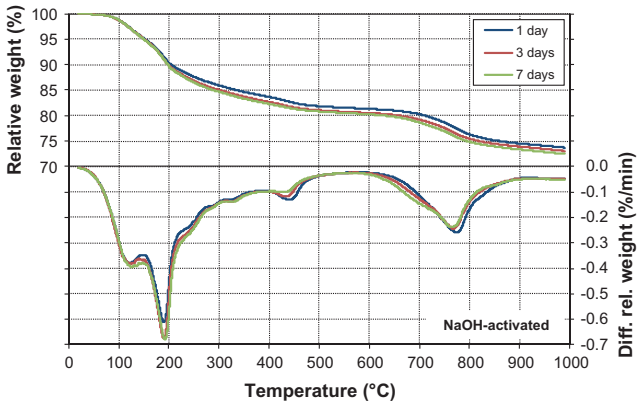

Fig. 9. TG/DTG curves of the NaOH-activated WSA after 1, 3 and 7 days of curing.

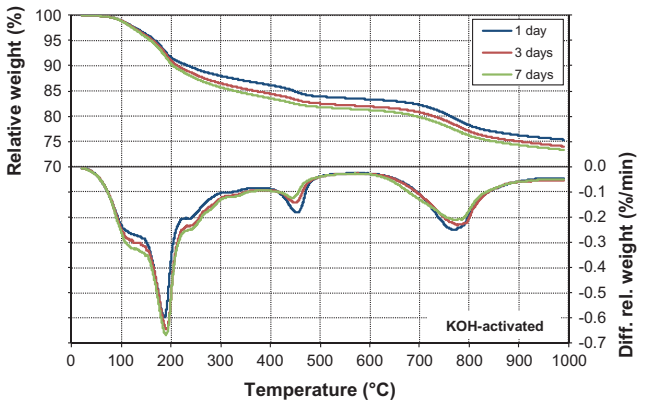

Fig. 10. TG/DTG curves of the KOH-activated WSA after 1, 3 and 7 days of curing.

water-activated paste (Fig. 4) shows that in the alkali-activated pastes the quantity of monocarbonate after 1 day of curing is considerably higher than in the water-activated pastes, while the amount of calcite is lower. In the further course of curing, only minor changes in the amounts of calcite and monocarbonate occurred in the alkali-activated pastes, confirming the XRD results. Somewhat more pronounced but still small changes were recorded for the amount of portlandite in both pastes (decreasing with curing time) and the height of the shoulder at 100–120 °C, attributed to C–S–H, for the KOH-activated paste (increasing with curing time). Summarizing, the thermogravimetric analyses show that in the NaOH- as well as in the KOH-activated paste the formation of monocarbonate proceeded significantly faster than for the water-activated paste until 1 day of curing but afterwards the hydration reactions took place much slower, almost ceasing.

The strength development of the alkali-activated pastes and mortars (Figs. 5 and 6, respectively) is quite different from that of the water-activated ones. A rapid increase of strength was observed, with compressive and flexural strengths about 2–6 times those of the water-activated materials after 1 day of hydration. Thereafter the strengths rose more slowly than in the water-activated materials, such that after 3–7 days of curing the strengths of the latter attain that of the alkali-activated WSA. Fig. 6 further shows that after that curing time compressive and flexural strength of the alkali-activated mortars remained virtually constant, while the compressive strength of the water-activated mortar was still increasing considerably. Significant differences between the behavior of the NaOH- and the KOH-activated materials were not observed.

4. Discussion

The WSA investigated in the present work contained calcite, lime, tricalcium aluminate, gehlenite, belite, quartz and talc as crystalline phases, which were found in WSA from other paper mills, as well [6,9–13]. However, depending on raw materials and processing conditions, the amounts of these phases differ and other phases may occur, thus, also the reaction products may vary. In the present study, calcite was present in the WSA at a relatively high quantity (~27%), compared to the ashes studied by most other investigators, but similar to one of the ashes studied by Davidenko et al. [13].

The high water demand of the WSA (insufficient workability of pastes at volume of liquid/mass of solid ratios lower than 1.00 cm^3 g^{-1}) is probably caused by its particle morphology, which is generally found to be irregular and porous for this kind of material [5,8,9,12]. In addition, the WSA may contain significant amounts of carbon as remnant from the combustion process (cf. [5]), which also would increase the water demand due to its high surface area. Mortars could be prepared at a somewhat lower liquid/solid ratio of 0.90 cm^3 g^{-1}; however, to achieve higher strengths and impermeability of mortars or concretes produced from it, a further reduction of the liquid/solid ratio has to be facilitated. This may be done by blending the WSA with suitable binder materials [6], optionally combined with the addition of superplasticizers [13].

The principle reaction product of the WSA, whether water- or alkali-activated, was monocarboaluminate. Calcium, aluminium and carbonate for the formation of the latter are provided by calcite, free lime (hydrated to give portlandite), tricalcium aluminate and also belite, whose fractions in the pastes decreased during hydration. Silicon for the formation of the smaller amounts of C–S–H, detected by TG/DTG, must have been mainly released by belite and probably by the glassy phase of the WSA, since gehlenite and quartz are known to be inert. The glassy phase may also contribute to calcium and aluminium release.

Neither ettringite (which is the sulfate-bearing hydrate expected to co-exist with monocarbonate [17,18]) nor any other sulfate-bearing phase was detected by XRD in any of the investigated pastes. Zhang and Glasser [19] observed that strong vacuum drying can lead to destruction of ettringite to an extent that it cannot be detected by XRD. However, these authors also found that drying to this point normally destroys AFm (monosulfoaluminate, "SO_4–AFm", in that case), as well. Based on the latter finding and since in our investigation monocarboaluminate gave clear reflections, we presume that, if ettringite would have been present at a significant amount, it would have led to distinguishable peaks in the diffractograms, too. Furthermore, solid solution between monocarboaluminate and monosulfoaluminate does not exist [18,20]. Thus, the sulfate contained in the WSA appears to be dissolved only to a small amount (i.e., existing in an sparingly soluble form), the amount of its reaction products accordingly being below the detection limit of the XRD analyses. However, the possibility of significant ettringite formation and its degradation during drying cannot completely ruled out. Despite the relatively high amount of alkalis in the NaOH- and KOH-activated pastes, also no alkali-bearing compounds were detected by XRD in the pastes, which parallels findings of Wang and Scrivener [21] for alkali-activated slag.

The main difference between the water- and the alkali-activated pastes was the temporal progress of the formation of reaction products and the strength development. In the NaOH- and KOH-activated pastes the formation of monocarboaluminate and the consumption of portlandite and calcite were much faster until the first day of curing than for the water-activated paste, but afterwards almost ceased. In line with this, the compressive strength of the alkali-activated WSA increased much more rapidly than that of the water-activated WSA until 1 day of curing but afterwards rose much slower, remaining practically constant after 7 days. On the contrary, the compressive strength of the water-activated mortar increased further after this period, although slower than before, and attains an about twice as high value after 28 days. Thus, in cases when rapid strength development is required, the use of alkalis for activation of the WSA is feasible, however, the maximum strength is then affected. This behavior should also be taken into account, if WSA is blended with materials containing high amounts of soluble alkalis, e.g. cement kiln dust. The flexural strengths were similar for all mortars after 28 days. This is attributed to the fact that, in addition to the amount of the main cementing phase monocarboaluminate, also the presence of flaws and microcracks strongly influences flexural strength.

The faster reaction and strength gain of the alkali-activated WSA is caused by the high alkalinity of the activating solution, which facilitates faster dissolution of the WSA. Regarding the stagnation of these processes after about 1 day, a mechanism analo-

gous to that observed for curing of Portland cement at elevated temperatures (40–50 °C) is assumed. Higher temperatures accelerate the hydration of cement, which causes higher strength in the first days of curing, compared to that of cement cured at ambient temperature. However, in the further course of curing, the strength of the latter exceeds that of the cement cured at elevated temperature. This is caused by the development of a dense rim of hydration products around the cement grains, the reason for this being the higher reaction rate than diffusion rate of the dissolved species at higher temperatures. This in turn hinders further reaction and leads to a more inhomogeneous microstructure with a higher fraction of large pores at elevated temperature-curing [16,22]. A comparable behavior has been observed with alkali-activated slag as well: When activated with NaOH or KOH, slag attains higher early compressive strength compared to slag, activated with sodium waterglass ($(Na_2O)(SiO_2)_x$), while at later age, the strength of the waterglass-activated material is much higher [23,24]. Also in that case, the slower long-term strength development, given by activation with alkali hydroxide solutions, is caused by formation of dense hydration products around the slag particles in the beginning, impacting on further hydration and thereby leading to a coarser, more porous microstructure [23,24]. Similarly, the accelerated reaction of the WSA in alkali solutions may lead to a dense rim of AFm and C-S-H around the WSA particles, by that impeding further dissolution and causing a more inhomogeneous microstructure with significantly lower compressive strength.

5. Conclusions

The WSA investigated in the present work consisted mainly of calcite, free lime, gehlenite, tricalcium aluminate, talc, quartz, some belite and probably a glassy phase. Hydration with water led to hydration of the free lime to give portlandite and rapid dissolution of the tricalcium aluminate, while portlandite and calcite dissolved continuously until 28 days of curing. The principle hydration product was monocarboaluminate, smaller amounts of C–S–H were also found. Parallel to the formation of monocarboaluminate, the strength of the water-activated paste and mortar increased continuously until 7 days of curing. Afterwards the strength gain was less rapid, but still significant.

Alkali-activation with 2 M NaOH or 2 M KOH solution led to a much more rapid formation of monocarboaluminate until 1 day of curing. Subsequently, the reaction and strength development proceeded slower than in the water-activated WSA, nearly ceasing after 7 days. This led to higher strengths after 1 day, but appreciably lower compressive strengths for the alkali-activated WSA after 28 days, compared to those of the water-activated WSA. This behavior of the alkali-activated WSA was tentatively attributed to the formation of a more inhomogeneous microstructure, analogous to the phenomena occurring with Portland cement, cured at elevated temperatures, and with slag, activated with alkali hydroxide solutions instead of waterglass. NaOH- and KOH-activated WSA behaved very similar, i.e. no significant influence of the kind of alkali ions in solution was observed.

Future research on the WSA should evaluate the validity of the proposed mechanism for the lower long-term strength of the alkali-activated WSA by use of scanning electron microscopy and/or mercury intrusion porosimetry. However, the presented results can already be used for a systematic selection of suitable alternative binder materials for blends with the WSA, in particular by considering the alkali content of the former. Equally important, knowledge about the reaction products of WSA is the basis for assessing the durability of these materials. For example, since monocarboaluminate is the main product of the investigated WSA, its chloride binding capacity is expected to be high, with little expansion caused by the chloride uptake [25]; on the other hand, ingress of sulfate will directly lead to the formation of ettringite [17,18]. By making use of this information, possible applications of WSA-based binders, e.g. in low grade concrete [6,8], road construction (soil stabilization) [11,12,26], mine backfill and waste stabilization/solidification [10], may be put into practice. In addition, the results can be used to improve the efficiency of the WSA as supplementary cementitious material in blends with Portland cement [9,13] by adjusting the amount of calcite introduced by the WSA to the cement composition, in particular the SO_3 and Al_2O_3 content [18,27].

Acknowledgements

The authors would like to thank K. Oppat, M. Delbove and T. Ihlenfeldt for their diligent assistance with the laboratory work.

References

[1] Monte MC, Fuente E, Blanco A, Negro C. Waste management from pulp and paper production in the European Union. Waste Manage 2009;29(1):293–308.
[2] Pera J, Amrouz A. Development of highly reactive metakaolin from paper sludge. Adv Cem Based Mater 1998;7(2):49–56.
[3] Vigil de la Villa R, Frías M, Sánchez de Rojas MI, Vegas I, García R. Mineralogical and morphological changes of calcined paper sludge at different temperatures and retention in furnace. Appl Clay Sci 2007;36(4):279–86.
[4] Frías M, Sánchez de Rojas MI, Rodríguez O, García Jiménez R, Vigil de la Villa R. Characterisation of calcined paper sludge as an environmentally friendly source of metakaolin for manufacture of cementitious materials. Adv Cem Res 2008;20(1):23–30.
[5] Koshikawa M, Isogai A. Analyses of incinerated ash of paper sludge: comparison with incinerated ash of municipal solid waste. J Mater Cycles Waste Manage 2004;6(1):64–72.
[6] Bai J, Chaipanich A, Kinuthia JM, O'Farrell M, Sabir BB, Wild S, et al. Compressive strength and hydration of wastepaper sludge ash-ground granulated blastfurnace slag blended pastes. Cem Concr Res 2003;33(8):1189–202.
[7] Mozaffari E, O'Farrell M, Kinuthia JM, Wild S. Improving strength development of wastepaper sludge ash by wet-milling. Cem Concr Compos 2006;28(2):144–52.
[8] Mozaffari E, Kinuthia JM, Bai J, Wild S. An investigation into the strength development of wastepaper sludge ash blended with ground granulated blastfurnace slag. Cem Concr Res 2009;39(10):942–9.
[9] Fava G, Ruello ML, Corinaldesi V. Paper mill sludge ash as supplementary cementitious material. J Mater Civ Eng 2011;23(6):772–6.
[10] Peyronnard O, Benzaazoua M. Estimation of the cementitious properties of various industrial by-products for applications requiring low mechanical strength. Resour Conserv Recycl 2011;56(1):22–33.
[11] Aubert JE, Segui P, Husson B, Measson M. A method developed to quantify lime and gypsum consumed by mineral additions. Cem Concr Compos 2012;34(7):874–80.
[12] Segui P, Aubert JE, Husson B, Measson M. Characterization of wastepaper sludge ash for its valorization as a component of hydraulic binders. Appl Clay Sci 2012;57:79–85.
[13] Davidenko T, Mikanovic N, Tagnit-Hamou A. Incompatibility issues between superplasticizers and wastepaper sludge ash. In: Tenth International Conference on Superplasticizers and Other Chemical Admixtures in Concrete, 2012 Oct 28-31, Prague, Czech Republic. Supplementary Papers, p. 37–48.
[14] Francois M, Renaudin G, Evrard O. A cementitious compound with composition $3CaO{\cdot}Al_2O_3{\cdot}CaCO_3{\cdot}11H_2O$. Acta Crystallogr C 1998;54(9):1214–7.
[15] Renaudin G, Francois M, Evrard O. Order and disorder in the lamellar hydrated tetracalcium monocarboaluminate compound. Cem Concr Res 1999;29(1):63–9.
[16] Lothenbach B, Winnefeld F, Alder C, Wieland E, Lunk P. Effect of temperature on the pore solution, microstructure and hydration products of Portland cement pastes. Cem Concr Res 2007;37(4):483–91.
[17] Kuzel H-J, Pöllmann H. Hydration of C_3A in the presence of $Ca(OH)_2$, $CaSO_4{\cdot}2H_2O$ and $CaCO_3$. Cem Concr Res 1991;21(5):885–95.
[18] Matschei T, Lothenbach B, Glasser FP. The AFm phase in Portland cement. Cem Concr Res 2007;37(2):118–30.
[19] Zhang L, Glasser FP. Critical examination of drying damage to cement pastes. Adv Cem Res 2000;12(2):79–88.
[20] Pöllmann H. Syntheses, properties and solid solution of ternary lamellar calcium aluminate hydroxi salts (AF_m-phases) containing SO_4^{2-}, CO_3^{2-} and OH^-. Neues Jahrb Mineral Abh 2006;182(2):173–81.
[21] Wang S-D, Scrivener KL. Hydration products of alkali activated slag cement. Cem Concr Res 1995;25(3):561–71.

[22] Kjellsen KO, Detwiler RJ, Gjørv OE. Backscattered electron imaging of cement pastes hydrated at different temperatures. Cem Concr Res 1990;20(2):308–11.
[23] Ben Haha M, Le Saout G, Winnefeld F, Lothenbach B. Influence of activator type on hydration kinetics, hydrate assemblage and microstructural development of alkali activated blast-furnace slags. Cem Concr Res 2011;41(3):301–10.
[24] Brough AR, Atkinson A. Sodium silicate-based, alkali-activated slag mortars: Part I. Strength, hydration and microstructure. Cem Concr Res 2002;32(6):865–79.
[25] Balonis M, Lothenbach B, Le Saout G, Glasser FP. Impact of chloride on the mineralogy of hydrated Portland cement systems. Cem Concr Res 2010;40(7):1009–22.
[26] Rahmat MN, Kinuthia JM. Effects of mellowing sulfate-bearing clay soil stabilized with wastepaper sludge ash for road construction. Eng Geol 2011;117(3–4):170–9.
[27] Matschei T, Lothenbach B, Glasser FP. The role of calcium carbonate in cement hydration. Cem Concr Res 2007;37(4):551–8.